

Signal of Quark Deconfinement in Millisecond Pulsars and Reconfinement in Accreting X-ray Neutron Stars

Norman K. Glendenning¹ and Fridolin Weber²

¹ Nuclear Science Division, & Institute for Nuclear and Particle Astrophysics,
Lawrence Berkeley National Laboratory,
University of California, Berkeley, CA 94720

² University of Notre Dame
Department of Physics
225 Nieuwland Science Hall
Notre Dame, IN 46556-5670

Abstract. Theoretically, the phase transition between the confined and deconfined phases of quarks can have a remarkable effect on the spin properties of millisecond pulsars and on the spin distribution of the population of x-ray neutron stars in low-mass binaries. In the latter class of stars, the effect has already been observed—a strong clustering in the population in a narrow band of spins. The observed clustering cannot presently be uniquely assigned to the phase transition as cause. However, there is another possible signal—not so far observed—in millisecond pulsars that we also discuss which would have the same origin, and whose discovery would tend to confirm the interpretation in terms of a phase transition in the stellar core.

1 Motivation

One of the great fascinations of neutron stars is the deep interior where the density is a few times larger than the density of normal nuclei. There, in matter inaccessible to us other than fleetingly in relativistic collisions, unfamiliar states may exist. The most exotic of these is, of course, quark matter—the deconfined phase of hadronic matter. It is quite plausible that ordinary canonical pulsars—those like the Crab, and more slowly rotating ones—have a quark matter core, or at least a mixed phase of quark and confined hadronic matter. If one were able to close pack nucleons to a distance such that they were touching at a radius of 0.5 fm, the density would be a mere $1/[(2r)^3\rho_0] = 6.5$ larger than normal nuclear density. If nucleons were close packed to their rms charge radius of 0.8 fm, the density would be 1.6 times nuclear density. Of course, fermions cannot be close packed according to the exclusion principle since their localization would give them enormous uncertainty in their momentum. They would be torn apart before they could be squeezed so much. This simple, and perhaps oversimplified argument, makes it plausible that ordinary (slowly rotating pulsars) have a quark matter core essentially from birth.

By comparison, millisecond (ms) pulsars are centrifugally flattened in the equatorial plane and the density is diluted in the interior. We shall suppose that

the critical phase transition density lies between the diluted density of millisecond pulsars and the high density at the center of canonical pulsars. Then as a millisecond neutron star spins down because it is radiating angular momentum in a broad band of electromagnetic frequencies as well as in a wind of particle-antiparticle pairs, or as a canonical neutron star at some stage begins accreting matter from a companion and is spun up, a change in phase of matter in the inner part of the star will occur.

Whatever the high density phase, and we assume here it is the quark deconfined one, it is softer than the normal phase. Otherwise no phase transition. Consequently, a change in the phase of matter will be accompanied by a change in the density distribution in the star. In the case of spindown of an isolated ms pulsar, the weight of the surrounding part of the star will squeeze the softer high density phase that is forming in the core. Conversely, an accreting neutron star that is being spun up, will spin out the already present quark phase. In either case, the star's moment of inertia will change, and therefore its spin rate will change to accommodate the conservation of angular momentum. Timing of pulsar and x-ray neutron star rotation is a relatively easy observation, and the effect of a phase change in the deep interior of neutron stars on timing or frequency distribution is what we study here.

The deconfinement or reconfinement of quark matter in a rotating star is a very slow process because it is governed by the rate of change of period, which is very small. This is an advantage. If the processes were fast, we would not likely witness the epoch of phase change, which is long, but nevertheless short (but not too short) compared to the timescales of spindown of ms pulsars or of spinup of accreting neutron stars in low-mass binaries. What we may see in the case of isolated ms pulsars is an occasional one that is spinning up, even though losing angular momentum to radiation. That would be a spectacular signal. What we may see in the case of accreting x-ray neutron stars in low-mass binaries is an unusual number of them falling within a small spin-frequency range—the range that corresponds to the spinout of the quark matter phase. That also is an easily observable signal. For stars of the same mass, the spontaneous spinup of isolated pulsars should occur at about the same spin frequency as the clustering in the population of neutron star accretors.

To place the canonical pulsars, ms pulsars, and x-ray accreting neutron stars in context, we refer to Fig. 1. Canonical pulsars have large surface magnetic fields, of the order of 10^{12} to 10^{13} G, and relatively long periods with an average of about 0.7 s. The ms pulsars have low fields, of the order of 10^8 to 10^9 G, and periods ranging from 1 to 10 ms. The x-ray stars that are accreting matter from a low-mass non-degenerate companion are believed to be the link [1,2,3,4] between the populations of canonical and ms pulsars—their path is indicated schematically in the figure. (Of course, defining ms pulsars to be those lying in the range of periods 1 to 10 ms is arbitrary.)

At present, fewer ms pulsars have been discovered than canonical pulsars. This is likely to be a selection effect. It is much more difficult to detect ms pulsars because there is radio noise in all directions (and therefore a possible signal)

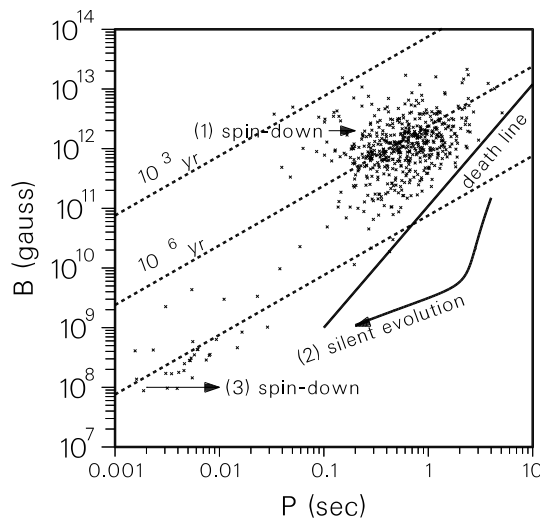


Fig. 1. Magnetic field of radio pulsars as a function of rotation period. Death line shows a combination of the two properties beyond which the beaming mechanism apparently fails. Canonical pulsars are designated as (1), millisecond pulsars as (3) and a schematic path for x-ray accreting neutron stars as (2). From Ref. [5].

and because of the dispersion by the interstellar electrons (from ionized hydrogen) of any pulsed signal which might be present in the direction the telescope is pointing. If present the signal is weak and contains a band of radio frequencies. Because of the different time-delay of each frequency, the frequencies are placed into a number of bins. For ms pulsars, the time-delay across the range of frequencies in a pulse is greater than the interval between pulses. Detection therefore depends on a tedious analysis that corrects the time-delay in each frequency bin for an assumed density of intervening interstellar gas; this is repeated for a succession of assumed densities. If the process converges to a periodic pulse, a pulsar has been discovered. Otherwise, the radio telescopes are pointed in a new direction. Systematically covering the sky is obviously very costly and time-consuming, and moreover, the present instrumentation is unable to detect pulsars with periods less than 1 millisecond.

2 Spontaneous Spinup of Millisecond Pulsar

We discuss here the effect that a change of phase in the core of a neutron star can have on the rotational properties of ms pulsars [6,7,8,9]. The analysis begins with the energy-loss equation for a rotating magnetized star whose magnetic axis is tilted with respect to the rotation axis. It is of historical interest to note that even before pulsars were discovered and soon identified with hypothetical

neutron stars, Pacini had postulated the existence of a highly magnetized rotating neutron star inside the Crab nebula as the energy source of the nebula and inferred some of the star's properties [10]. It was already known before 1967 that the nebula, formed in a supernova in 1054, is being accelerated and illuminated by a power source amounting to $\sim 4 \times 10^{38}$ erg/s. This compares with a solar luminosity of $L_{\odot} \sim 4 \times 10^{33}$ erg/s. The power output of the rotating Crab pulsar equals that of 100,000 suns. Equating the power input to the nebula with the power radiated by a rotating magnetic dipole,

$$4 \times 10^{38} \text{ ergs/s} = -\frac{dE}{dt} = -\frac{d}{dt} \left(\frac{1}{2} I \Omega^2 \right) = \frac{2}{3} R^6 B^2 \Omega^4 \sin^2 \alpha, \quad (1)$$

and knowing the period and rate of change of period of the pulsar,

$$P \sim \frac{1}{30} \text{ s}, \quad \dot{P} \sim 4 \times 10^{-13} \text{ s/s}, \quad (2)$$

the moment of inertia, surface magnetic field strength, and rotational energy of the Crab pulsar can be inferred as

$$\begin{aligned} I &\sim 9 \times 10^{44} \text{ g cm}^2 \sim 70 \text{ km}^3, \\ B &\sim 4 \times 10^{12} \text{ gauss}, \\ E_{\text{rot}} &\sim \frac{1}{2} I \Omega^2 \sim 2 \times 10^{49} \text{ ergs} \sim 10^{55} \text{ MeV}. \end{aligned} \quad (3)$$

For these estimates, we have assumed that $\sin \alpha = 1$, where α is the angle between magnetic and rotational axis. (Gravitational units $G = c = 1$ are used frequently. For convenient conversion formula to other units see ch. 3 of Ref. [5].)

Returning to the effect that a phase change can have on the rotational properties of a pulsar through changes in the moment of inertia induced by a phase transition, we rewrite Eq. (1) in greater generality:

$$\dot{E} = \frac{d}{dt} \left(\frac{1}{2} I \Omega^2 \right) = -C \Omega^{n+1}. \quad (4)$$

Here we have written for convenience

$$C = (2/3) R^6 B^2 \sin^2 \alpha. \quad (5)$$

We find the deceleration equation

$$\dot{\Omega} = -\frac{C}{I} \Omega^n \left(1 + \frac{I' \Omega}{2I} \right)^{-1}. \quad (6)$$

In work previous to ours, $I' \equiv dI/d\Omega$ was assumed to vanish. This would be a good approximation for canonical pulsars but not for millisecond pulsars.

The angular momentum of a rotating star in General Relativity can be obtained numerically as a solution of Einstein's equations or as a very complicated algebraic expression in a perturbative expansion. The moment of inertia is then obtained as $I = J/\Omega$. The complication arises in two ways. First, a rotating star

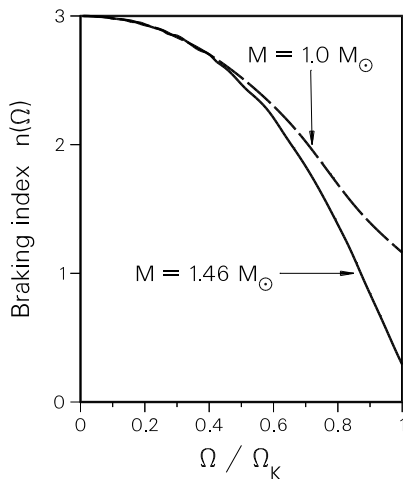


Fig. 2. Apparent braking index for pure dipole radiation ($n = 3$) as function of rotational frequency for stars of two different masses containing hyperons (but no first order phase transition). (The mass indicated is for slow rotation.)

sets the local inertial frames into rotation. This is referred to as frame dragging. Second, the structure of the rotating star depends on the frame dragging frequency, ω , which is position dependent, and on the spacetime metric, which also depends on ω . Algebraic expressions were obtained in Refs. [11,9].

The index n in equation Eq. (4) equals three for magnetic dipole radiation. In principle, it can be measured in terms of the frequency Ω and its first two time derivatives. But the dependence of I on Ω introduces a correction so that the dimensionless *measurable* braking index is given by

$$n(\Omega) = \frac{\Omega \ddot{\Omega}}{\dot{\Omega}^2} = n - \frac{3I'\Omega + I''\Omega^2}{2I + I'\Omega}. \quad (7)$$

So the measurable braking index will differ from 3 for ms pulsars, if for no other reason than that the centrifugal deformation of the star relaxes as the star spins down. Such a dependence on Ω is illustrated in Fig. 2

It is especially noteworthy that the *magnitude* of the signal—the deviation of $n(\Omega)$ from n —depends on $dI/d\Omega$ which is large, especially for millisecond pulsars, but the *duration* of the signal depends on $d\Omega/dt$ which is small. Therefore, the variation of the braking index over time is very slow, the time-scale being astronomical. So what one would observe over any observational era is a constant braking index $n(\Omega)$ that is less (if no phase transition) than the n characteristic of the energy-loss mechanism Eq. (4) even if the radiation were a pure multipole. We will see that the effect of a phase transition on the measurable braking index can be (but not necessarily) much more dramatic. (We distinguish between the constant $n = 3$ of the energy-loss equation and the measurable quantity of Eq. (7).)

We turn now to our original postulate—that canonical pulsars have a quark matter phase in their central region but that ms pulsars which are centrifugally diluted, do not. In the slow course of spindown the central density will rise however. When the critical density is reached, stiff nuclear matter will be replaced slowly in the core by highly compressible quark matter. The overlaying layers of nuclear matter weigh down on the core and compress it. Its density rises. The star shrinks—mass is redistributed with growing concentration at the center. The by-now more massive central region gravitationally compresses the outer nuclear matter even further, amplifying the effect. The density profile for a star at three angular velocities, (1) the limiting Kepler angular velocity at which the star is stretched in the equatorial plane and its density is centrally diluted, (2) an intermediate angular velocity, and (3) a non-rotating star, are shown in Fig. 3. We see that the central density rises with decreasing angular velocity by a factor of three and the equatorial radius decreases by 30 percent. In contrast, for a model for which the phase transition did not take place, the central density would change by only a few percent [12]. The phase boundaries are shown in Fig. 4 from the highest rotational frequency to zero rotation.

The redistribution of mass and shrinkage of the star change its moment of inertia and hence the characteristics of its spin behavior. The star must spin up to conserve angular momentum which is being carried off only slowly by the weak electromagnetic dipole radiation. The star behaves like an ice skater who goes into a spin with arms outstretched, is slowly spun down by friction, temporarily spins up by pulling the arms inward, after which friction takes over again.

The behavior of the moment of inertia in the vicinity of the critical region of growth of the quark matter core is shown in Fig. 5. The critical period of rotation is $P = 2\pi/\Omega \sim 4.6$ ms. Much the same phenomenon was observed in rotational nuclei during the 1970s [13,14] and had been predicted by Mottelson and Valatin [15] though of course the phase changes are different (see Fig. 6). The mechanism is evidently quite robust, but it need not occur in every model star. In the present instance, the mass of the neutron star is very close to the limiting mass of the non-rotating counterpart. This does not necessarily mean that it will be a rare event. The mass of neutron stars is bounded from below by the Chandrasekhar mass limit which is established by electron pressure and has a value of $\sim 1.4M_\odot$. The limiting mass of neutron stars may be very little more because of the softening of the nuclear equation of state by hyperonization and quark deconfinement. This could be the reason that neutron star masses seem to lie in a very small interval [5].

As already pointed out, the progression in time of the growth of the quark core is very slow, being governed by the weak processes that cause the loss of angular momentum to radiation. Using the computed moment of inertia for a star of constant baryon number as shown in Fig. 5 we can integrate Eq. (6) to find the epoch of spinup to endure for 2×10^7 y. This is a small but significant fraction of the spin-down time of ms pulsars which is $\sim 10^9$ y. So if ms pulsars are near their limiting mass and are approximately described by our model, about 1 in 50 *isolated* ms pulsars should be spinning up instead of spinning down.

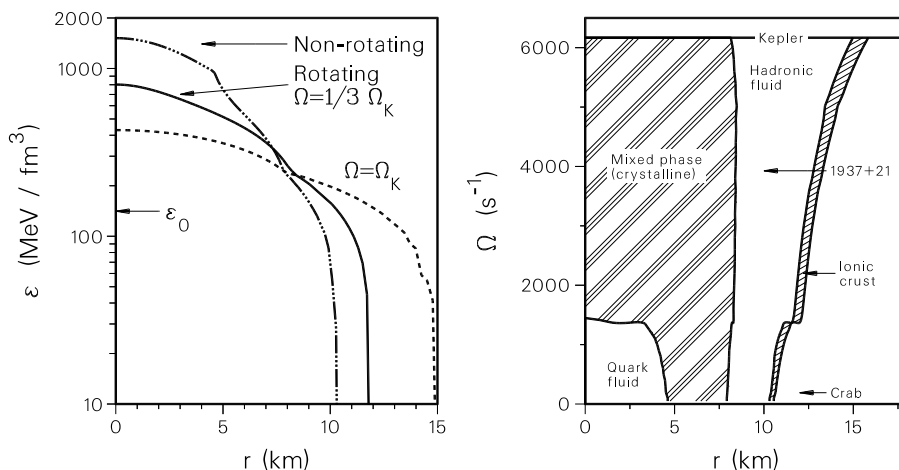


Fig. 3. Mass profiles as a function of equatorial radius of a star rotating at three different frequencies, as marked. At low frequency the star is very dense in its core, having a 4 km central region of highly compressible pure quark matter. At intermediate frequency, the pure quark matter phase is absent and the central 8 km is occupied by the mixed phase. At higher frequency (nearer Ω_K) the star is relatively dilute in the center and centrifugally stretched. Inflections at $\epsilon = 220$ and 950 are the boundaries of the mixed phase.

Fig. 4. Radial boundaries at various rotational frequencies separating (1) pure quark matter, (2) mixed phase, (3) pure hadronic phase, (4) ionic crust of neutron rich nuclei and surface of star. The pure quark phase appears only when the frequency is below $\Omega \sim 1370$ rad/s. Note the decreasing radius as the frequency falls. The frequencies of two pulsars, the Crab and PSR 1937+21 are marked for reference.

Presently, about 60 ms pulsars have been identified, and about half of them are isolated, the others being in binary systems. Because the period of ms pulsars can be measured with an accuracy that rivals atomic clocks, identification of the direction of change of period would not take long. For example, PSR1937+21 has a period (measured on 29 November 1982 at 1903 UT)

$$P = 1.5578064487275(3) \text{ ms}.$$

Its rate of change of period is a mere $\dot{P} \sim 10^{-19}$. But because of the high accuracy of the period measurement, it would take only two measurements spaced 0.3 hours apart to detect a unit change in the last significant figure, and hence to detect in which direction the period is changing.

In principal, the period and first two time derivatives can be measured. The dimensionless ratio formed from them yields the braking index n of the energy-loss mechanism, corrected by a term that depends on changes in the moment of inertia. In the case that a phase change causes a spinup of the pulsar, as in

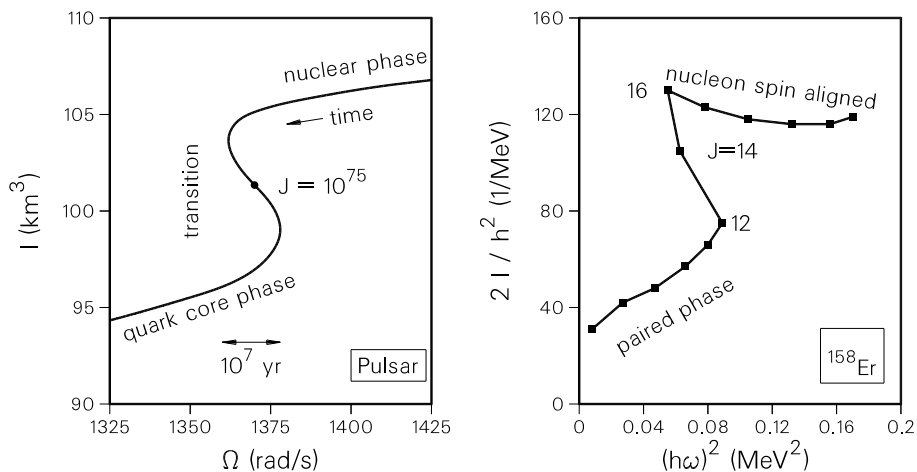


Fig. 5. Moment of inertia of a neutron star at angular velocities for which the central density rises from below to above critical density for the pure quark matter phase as the centrifugal force decreases. Time flows from large to small I . The most arresting signal of the phase change is the spontaneous spin-up that an isolated pulsar would undergo during the growth in the region of pure quark matter. (Adapted from Ref. [6].)

Fig. 6. Nuclear moment of inertia as a function of squared frequency for ^{158}Er , showing backbending in the nuclear case. Quantization of spin yields the unsmooth curve compared to the one in Fig. 5.

Fig. 5, the measurable dimensionless quantity $n(\Omega)$ has two singularities at the frequencies at which $dI/d\Omega$ switches between $\pm\infty$. From Eq. (6) it is clear that $\dot{\Omega}$ will pass through zero and change sign at both turning points. Therefore, the measurable braking index Eq. (7) will have singularities as shown in Fig. 7. The braking index with a nominal value of 3 will make enormous excursions from that value. The braking index is shown in Fig. 8 over one decade in time, and has an anomalous value for 10^8 y. However, the second time derivative has never been measured for a ms pulsar because the rate of change of frequency is so slow. So the one, and easily observable signal, is the spontaneous spinup of an isolated ms pulsar. Such a pulsar has not yet been observed. But then, only about 30 isolated ms pulsars have so far been detected, whereas, according to our estimate, only 1 in 50 ms pulsars of mass close to the maximum would presently be passing through the epoch in which a quark matter core grows.

We briefly describe the nuclear and quark matter phases used in this and the following sections. More details can be found in the Appendix and in Ref. [6]. The initial mass of the star in our examples is $1.42M_{\odot}$. Briefly, confined nuclear matter is described by a covariant Lagrangian describing the interaction of the members of the baryon octet with scalar, vector and vector-isovector mesons and

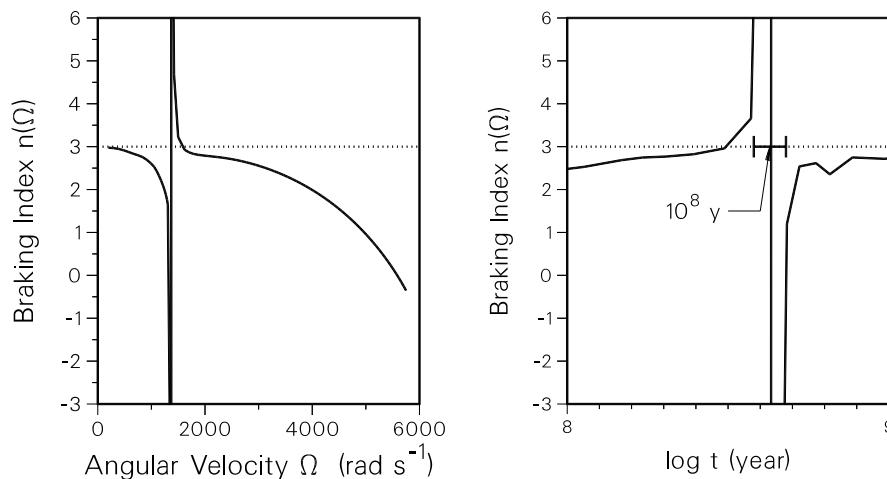


Fig. 7. Braking index for a pulsar that passes through a change of phase in the central region as a function of angular velocity.

Fig. 8. Braking index as a function of time over one decade in the critical region in case of a phase transition in the interior of the star. (From Ref. [7].)

solved in the meanfield approximation. Quark matter is described by the MIT bag model.

3 Accreting X-ray Neutron Stars in Binaries

Some neutron stars have non-degenerate companions. Such neutron stars are radio silent because a wind from the hot surface of the companion disperses the pulsed radio signal which a rotating magnetized neutron star would otherwise radiate into space. Late in the life of the neutron star, when the slowly evolving companion begins to overflow the Roche lobe, mass transfer onto the neutron star commences. The drag of the magnetic dipole torque will be eclipsed by the transfer of mass and angular momentum onto the neutron star. It has begun its evolution from an old slowly rotating neutron star with long period and high magnetic field, to a ms pulsar with low field (sometimes referred to as a “recycled pulsar”). During the long intermediate stage, when the surface and accretion ring are heated to high temperature, the star radiates x-rays.

Any asymmetry in the mass accretion pattern will cause a variability in x-ray emission. At an accretion rate of $10^{-9}M_{\odot}/y$ it would take only 10^8 y to spin up the neutron star to a period of 2 ms (500 Hz). Consequently, millisecond variability in the x-ray luminosity is expected and observed.

Accreting x-ray neutron stars provide a very interesting contrast to the spin-down of isolated ms pulsars [16]. Presumably they are the link between the

canonical pulsars with mean period of 0.7 sec and the ms pulsars [1,2,3,4]. If the critical deconfinement density falls within the range spanned by canonical pulsars, quark matter will already exist in them but may be “spun” out of x-ray stars as their rotational frequency increases during accretion. We can anticipate that in a certain frequency range, the changing radial extent of the quark matter phase will actually inhibit changes in frequency because of the increase in moment of inertia occasioned by the gradual disappearance of the quark matter phase. Accreters will tend to spend a greater length of time in the critical frequencies than otherwise. There will be an anomalous number of accreters that appear at or near the same frequency. This is what was found recently in data obtained with the Rossi X-ray Timing Explorer (RXTE). For an extensive review of the discoveries made in the short time since this satellite was launched (1995), see Ref. [17].

The spinup evolution of an accreting neutron star is a more complicated problem than that of the spindown of an isolated ms pulsar of constant baryon number. It is complicated by the accretion of matter ($\dot{M} \gtrsim 10^{-10} M_\odot \text{ yr}^{-1}$), a changing magnetic field strength (from $B \sim 10^{12}$ to $\sim 10^8$ G), and the interaction of the field with the accretion disk.

The change in moment of inertia as a function of rotational frequency caused by spinup due to accretion is similar to that described in the previous section, but in reverse [6]. However, there are additional phenomena as just mentioned. The spin-up torque of the accreting matter causes a change in the star’s angular momentum according to the relation [18,19,20]

$$\frac{d}{dt} J \equiv \frac{d}{dt} (I\Omega) = N_A(r_m) - N_M(r_c). \quad (8)$$

The first term on the right-hand-side is the torque exerted on the star by a mass element rotating at the base of the accretion disk with Keplerian velocity ω_K . Denoting this distance with r_m , one readily finds that $N_A(r_m)$ is given by ($G = c = 1$)

$$\begin{aligned} N_A(r_m) &= r_m^2 \dot{M} \omega_K \\ &= r_m^2 \dot{M} \left(\frac{M}{r_m^3} \right)^{1/2} \\ &= \dot{M} \sqrt{Mr_m} \equiv \dot{M} \tilde{l}(r_m), \end{aligned} \quad (9)$$

where \dot{M} stands for the accretion rate, and $\tilde{l}(r_m)$ is the specific angular momentum of the accreting matter (angular momentum added to the star per unit mass of accreted matter). The second term on the right-hand-side of Eq. (8) stands for the magnetic plus viscous torque term ($\kappa \sim 0.1$),

$$N_M(r_c) = \kappa \mu^2 r_c^{-3}, \quad (10)$$

with $\mu \equiv R^3 B$ the star’s magnetic moment. Upon substituting Eqs. (9) and (10) into (8) and writing the time derivative $d(I\Omega)/dt$ as $d(I\Omega)/dt = (dI/dt)\Omega +$

$I(d\Omega/dt)$, the time evolution equation for the angular velocity Ω of the accreting star can be written as

$$I(t)\frac{d\Omega(t)}{dt} = \dot{M}\tilde{l}(t) - \Omega(t)\frac{dI(t)}{dt} - \kappa\mu(t)^2 r_c(t)^{-3}. \quad (11)$$

The quantities r_m and r_c denote fundamental length scales of the system. The former, as mentioned above, denotes the radius of the inner edge of the accretion disk and is given by ($\xi \sim 1$)

$$r_m = \xi r_A. \quad (12)$$

The latter stands for the co-rotating radius defined as

$$r_c = (M\Omega^{-2})^{1/3}. \quad (13)$$

Accretion will be inhibited by a centrifugal barrier if the neutron star's magnetosphere rotates faster than the Kepler frequency at the magnetosphere. Hence $r_m < r_c$, otherwise accretion onto the star will cease. A further fundamental lengthscale is set by the Alfvén radius r_A , which enters in Eq. (12). It is the radius at which the magnetic energy density, $B^2(r)/8\pi$, equals the total kinetic energy density, $\rho(r)v^2(r)/2$, of the accreting matter. For a dipole magnetic field outside the star of magnitude

$$B(r) = \frac{\mu}{r^3}, \quad (14)$$

this condition reads

$$\frac{1}{8\pi}B^2(r_A) = \frac{1}{2}\rho(r_A)v^2(r_A), \quad (15)$$

where $v(r_A)$ is of the order of the Keplerian velocity, or, which is similar, the escape velocity at distance r_A from the neutron star,

$$v(r_A) = \left(\frac{2M}{r_A}\right)^{1/2}. \quad (16)$$

The density $\rho(r_A)$ in Eq. (15) can be replaced by

$$\rho(r_A) = \frac{\dot{M}}{4\pi r_A^2 v^2(r_A)}, \quad (17)$$

which follows from the equation of continuity. With the aid of Eqs. (14), (16) and (17), one obtains from (15) for the Alfvén radius the following expression:

$$r_A = \left(\frac{\mu^4}{2M\dot{M}^2}\right)^{1/7}. \quad (18)$$

It is instructive to write this equation as

$$r_A = 7 \times 10^3 \dot{M}_{-10}^{-2/7} \mu_{30}^{4/7} \left(\frac{M}{M_\odot}\right)^{-1/7} \text{ km}, \quad (19)$$

where $\dot{M}_{-10} \equiv \dot{M}/(10^{-10} M_{\odot} \text{ yr}^{-1})$ and $\mu_{30} \equiv \mu/(10^{30} \text{ G cm}^3)$. It shows that canonical accreters ($\dot{M}_{-10} = 1$) with strong magnetic fields of $B \sim 10^{12} \text{ G}$ have Alfvén radii, and thus accretion disks, that are thousands of kilometers away from their surfaces. This is dramatically different for accreters whose magnetic fields have weakened over time to values of $\sim 10^8 \text{ G}$, for instance. In this case, the Alfvén radius has shrunk to $\sim 40 \text{ km}$, which is just a few times the stellar radius.

We assume that the magnetic field evolves according to

$$B(t) = B(\infty) + [B(0) - B(\infty)]e^{-t/t_d} \quad (20)$$

with $t = 0$ at the start of accretion, and where $B(0) = 10^{12} \text{ G}$, $B(\infty) = 10^8 \text{ G}$, and $t_d = 10^6 \text{ yr}$. Such a decay to an asymptotic value seems to be a feature of some treatments of the magnetic field evolution of accreting neutron stars [21]. Moreover, it expresses the fact that canonical neutron stars have high magnetic fields and ms pulsars have low fields (see Fig. 1). Beyond that, as just mentioned, the condition that accretion can occur demands that $r_m < r_c$ which inequality places an upper limit on the magnitude of the magnetic field of ms neutron star accreters of 2 to $6 \times 10^8 \text{ G}$ [3].

Frequently, it has been assumed that the moment of inertia in Eq. (11) does not respond to changes in the centrifugal force, and in that case, the above equation yields a well-known estimate of the period to which a star can be spun up [2]. The approximation is true for slow rotation. However, the response of the star to rotation becomes increasingly important as the star is spun up. Not only do changes in the distribution of matter occur but internal changes in composition occur also because of changes induced in the central density by centrifugal dilution [6]; both changes effect the moment of inertia and hence the response of the star to accretion.

The moment of inertia of ms pulsars or of neutron star accreters has to be computed in GR without making the usual assumption of slow rotation [22,23]. We use a previously obtained expression for the moment of inertia of a rotating star, good to second order in Ω [11]. The expression is too cumbersome to reproduce here. Stars that are spun up to high frequencies close to the breakup limit (Kepler frequency) undergo dramatic interior changes; the central density may change by a factor of four or so over that of a slowly rotating star if a phase change occurs during spin-up (cf. Fig. 3) [7,24].

Figure 9 shows how the moment of inertia changes for neutron stars in binary systems that are spun up by mass accretion according to Eq. (11) until $0.4M_{\odot}$ has been accreted. The neutron star models are fully described in Ref. [6] and references therein and briefly in the Appendix of this article. The initial mass of the star in our examples is $1.42M_{\odot}$. In one case, it is assumed that a phase transition between quark matter and confined hadronic matter occurs, and in the other that it does not. This accounts for the different initial moments of inertia, and also, as we see, the response to spinup. Three accretion rates are assumed, which range from $\dot{M}_{-10} = 1$ to 100 (where \dot{M}_{-10} is measured in units of $10^{-10}M_{\odot}$ per year). These rates are in accord with observations made on low-mass X-ray binaries (LMXBs) observed with the Rossi X-ray Timing Explorer

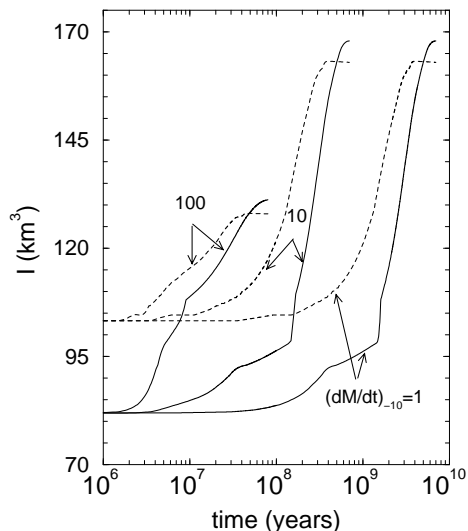


Fig. 9. Moment of inertia of neutron stars as a function of time with (solid curves) and without (dashed curves) quark matter core assuming $0.4M_{\odot}$ is accreted. Results for three average accretion rates are illustrated.

[17]. The observed objects, which are divided into Z sources and A(toll) sources, appear to accrete at rates of $\dot{M}_{-10} \sim 200$ and $\dot{M}_{-10} \sim 2$, respectively. Although in a given binary, \dot{M} varies on a timescale of days, we take it to be the constant average rate in our calculations.

Figure 10 shows the spin evolution of accreting neutron stars as determined by the changing moment of inertia and the spin evolution equation, Eq. (11). Neutron stars *without* quark matter in their centers are spun up along the dashed lines to equilibrium frequencies between about 600 Hz and 850 Hz, depending on accretion rate and magnetic field. The dI/dt term for these sequences manifests itself only insofar as it limits the equilibrium periods to values smaller than the Kepler frequency, ν_K . In both Figs. 9 and 10 we assume that $0.4M_{\odot}$ is accreted. Otherwise, the maximum frequency attained is less, the less matter is accreted.

The spin-up scenario is dramatically different for neutron stars in which a first order phase transition occurs. In this case, as known from Fig. 9, the temporal conversion of quark matter into its mixed phase of quarks and confined hadrons is accompanied by a pronounced increase of the stellar moment of inertia. This increase contributes so significantly to the torque term $N(r_c)$ in Eq. (11) that the spinup rate $d\Omega/dt$ is driven to a plateau around those frequencies at which the pure quark matter core in the center of the neutron star gives way to the mixed phase of confined hadronic matter and quark matter. The star resumes ordinary spin-up when this transition is completed. The epoch during which the spin rates reach a plateau are determined by attributes like the accretion rate, magnetic field, and its assumed decay time. The epoch lasts between $\sim 10^7$ and 10^9 yr depending on the accretion rate at the values taken for the other factors.

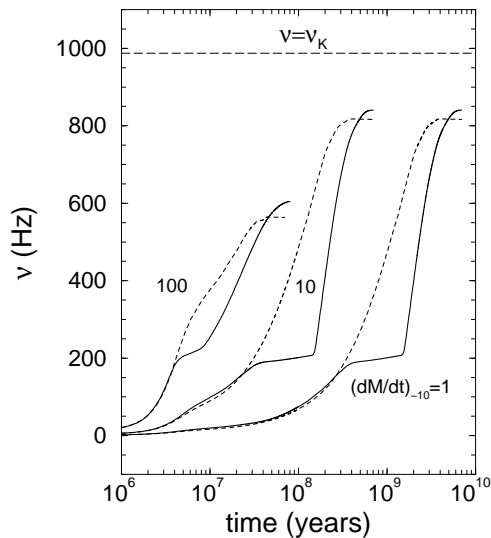


Fig. 10. Evolution of spin frequencies ($\nu \equiv \Omega/2\pi$) of accreting neutron stars with (solid curves) and without (dashed curves) quark deconfinement if $0.4M_{\odot}$ is accreted. (If the mass of the donor star is less, then so is the maximum attainable frequency.) The spin plateau around 200 Hz signals the ongoing process of quark confinement in the stellar centers. Note that an equilibrium spin is eventually reached which is less than the Kepler frequency.

We can translate the information in Fig. 10 into a frequency distribution of X-ray stars by assuming that neutron stars begin their accretion evolution at the average rate of one per million years. A different rate will only shift some neutron stars from one bin to an adjacent one, but will not change the basic form of the distribution. The donor masses in the binaries are believed to range between 0.1 and $0.4M_{\odot}$. For lack of more precise knowledge, we assume a uniform distribution of donor masses (or mass accreted) in this range and repeat the calculation shown in Fig. 10 at intervals of $0.1M_{\odot}$.

The result for the computed distribution of rotational frequency of x-ray neutron stars is shown in Fig. 11; it is striking. Spinout of the quark matter core as the neutron star spins up is signalled by a spike in the distribution which would be absent if there were no phase transition in our model of the neutron star. We stress that what we plot is our prediction of the *relative* frequency distribution of the *underlying* population of x-ray neutron stars—but the weight given to the spike as compared to the high frequency tail depends sensitively on the weight with which the donor masses are assigned and the initial mass distribution of neutron stars in LMXBs. As already mentioned, we give equal weight to donor masses between 0.1 and $0.4M_{\odot}$ and the initial mass of the neutron star is $1.42M_{\odot}$. The objects above 400 Hz in Fig. 11 are actually unstable and will collapse to black holes. Donors of all masses in the range just mentioned

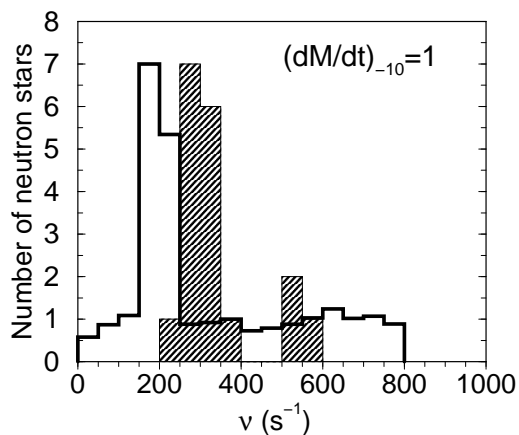


Fig. 11. Frequency distribution of X-ray neutron stars. Calculated distribution (open histogram) for the underlying population is normalized to the number of observed objects (18) at the peak. (The normalization causes a fractional number to appear in many bins of the calculated distribution.) Data on neutron stars in LMXBs (shaded histogram) is from Ref. [17]. See text and especially the reference for caveats to the interpretation. The spike in the calculated distribution corresponds to the spinout of the quark matter phase and the corresponding growth of the moment of inertia as compressible quark matter is replaced by relatively incompressible nuclear matter. Otherwise the spike would be absent.

contribute to neutron stars of spin up to 400 Hz. Neutron stars of lower initial mass than our $1.42M_{\odot}$ with donors of mass at the higher end of their range will produce spins above 400 Hz. In other words, the relative population in the peak as compared to the background will be sensitive to the unknown factors (1) accretion rate (2) initial mass distribution of neutron stars in LMXBs (3) mass distribution of donor stars. However, the position of the peak in the spin distribution of x-ray neutron stars is a property of nuclear matter and independent of the above unknowns.

The calculated concentration in frequency of x-ray neutron stars is centered around 200 Hz; this is about 100 Hz lower than the observed spinup anomaly (see discussion below). This discrepancy should not be surprising in view of our total ignorance¹ of the equation of state above saturation density of nuclear matter and the necessarily crude representation of hadronic matter in the two phases in the absence of relevant solutions to the fundamental QCD theory of strong interactions. We represent the confined phase by relativistic nuclear field theory and the deconfined phase by the MIT bag model. However crude these or any other models of hadronic matter may be, the physics underlying the effect of a phase transition on spin rate is robust, although not inevitable. We have

¹ There are upcoming radioactive beam experiments from which it is hoped to gain information on the equation of state of asymmetric nuclear matter [25,26,27].

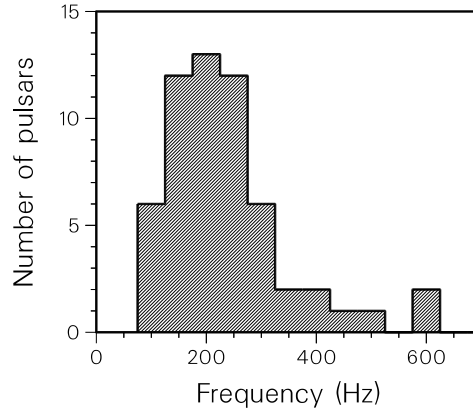


Fig. 12. Data on frequency distribution of millisecond pulsars ($1 \leq P < 10$ ms). Frequency bins are 50 Hz wide.

cited the example of an analogous phenomenon found in rotating nuclei in the previous section.

The data that we have plotted in Fig. 11 is gathered from Tables 2, 3, and 4 of the review article of van der Klis concerning discoveries made with the Rossi X-ray Timing Explorer, launched near the end of 1995 [17]. The interpretation of millisecond oscillations in the x-ray emission, either that found in bursts or of the difference between two observed quasi-periodic oscillations (QPOs) in x-ray brightness, is ambiguous in some cases. In particular, the highest frequency near 600 Hz in the “observed” data displayed in our figure, may actually be twice the rotational frequency of the star [17]. The millisecond variability in x-ray phenomena associated with accretion onto neutron stars that has been observed since the launch of the satellite was anticipated several decades ago. However, the consistency of the phenomena from one binary to another raises questions about interpretation. In this sense, the field is quite young. We refer to the above cited review article for details and references to the extensive literature.

Nevertheless, the basic feature will probably survive—a clustering in rotational frequencies of x-ray neutron stars and a higher frequency tail. Certainly there are high frequency *pulsars*. A histogram of *ms pulsar* frequencies shows a broad distribution around 200 Hz, and a tail extending to ~ 600 Hz as shown in Fig. 12. So both the (sparse) data on X-ray objects and on ms pulsars seem to agree on a peak in the number of stars at moderately high rotational frequency and on an attenuation at high frequency. For ms pulsars, however, the attenuation at high frequency may be partly a selection effect due to interstellar dispersion of the radio signal.

There have been other suggestions as to the cause of the spike, several of which we cite (c.f. [28,29,30]). These works are concerned with the balance of the spinup torque by a gravitational radiation torque. Our proposal has several merits: (1) the mechanism involving a change in moment of inertia triggered by

a phase transition in the stellar core due to changing density profile in the star as its spin changes is robust—it is known to occur in rotating nuclei; (2) The phase transition should occur in reverse in isolated ms pulsars and in neutron star accretors and at about the same frequency for similar mass stars; (3) The phase transition causes accretion induced spinup to stall for a long epoch, but to resume after the quark core has been expelled, thus accounting for high spin objects like very fast ms pulsars as well as the clustering in spin of the population of accretors.

4 Evolution from Canonical to Millisecond Pulsar

In the foregoing we have discussed possible signals of a phase transition in isolated ms pulsars and in accreting x-ray neutron stars in binary orbit with a low-mass companion. Spinup by mass accretion is believed to be the pathway from the relatively slowly rotating canonical pulsars formed by conservation of angular momentum in the core collapse of massive stars, and the rapidly rotating millisecond pulsars [1,2]. In this section we trace some of the possible evolutionary routes under the various physical conditions under which accretion occurs [31].

The evolutionary track between canonical and ms pulsars in the coordinates of magnetic field strength and rotational period (refer to Fig. 1) will depend on the rate of mass accretion, its duration, the centrifugal change in the moment of inertia of the star, the strength of the magnetic field and timescale of its decay, and possibly other affects. Many papers have been devoted to the decay of the magnetic field. It is an extremely complicated subject, with many physical uncertainties such as the actual location of the field, whether in the core or crust, the degree to which the crust is impregnated with impurities, crustal heating and resultant reduction in conductivity and therefore increase in ohmic field decay, screening of the magnetic field by accreted material, and so on.

The field is believed to decay only weakly due to ohmic resistance in canonical pulsars, but very significantly if in binary orbit with a low-mass non-degenerate star, when the companion fills its Roche lobe. This era can last up to 10^9 y and cause field decay by several orders of magnitude. For a review of the literature and several evolutionary scenarios, see Refs. [20,21,32,33,34].

While there is no consensus concerning the magnetic field decay, observationally, we know that canonical pulsars have fields of $\sim 10^{11}$ to $10^{13}G$, while millisecond pulsars have fields that lie in the range $\sim 10^8$ to 10^9G . We shall rely on this observational fact, and assume that the field decays according to Eq. (20). where $B(\infty) = 10^8$ G, $B(0) = 10^{12}$ G and $t_d = 10^5$ to 10^7 yr. Moreover, this is the general form found in some scenarios [21]. However, we shall also make a comparison with a purely exponential decay.

There are three distinct aspects to developing an evolutionary framework. One has to do with the accretion process itself, which has been developed by a number of authors in the framework of classical physics([18,19,20]) and which we employed in the previous section. Another has to do with the field decay, which

The initial conditions for the evolution are arbitrary to a high degree. Canonical pulsars have a broad range of magnetic field strengths. The period of the pulsar at the time that the companion overflows its Roche lobe and accretion commences is also arbitrary. Any observed sample of x-ray accreters presumably spans a range in these variables. For concreteness, we assume that the pulsar has a field of 10^{12} G and that the period of the pulsar is 1 ms when accretion begins. The donor mass in the low-mass binaries are in the range 0.1 to $0.4M_{\odot}$. Our sample calculations are for accretion of up to $0.4M_{\odot}$.

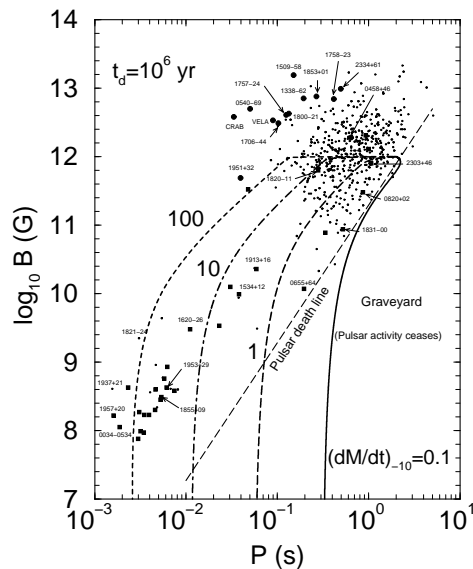


Fig. 14. Evolutionary tracks traced by neutron stars in the X-ray accretion stage, beginning on the death line with purely exponential decay of the B field. As in Fig. 13, $t_d = 10^6$ yr.

We find essentially a continuum of evolutionary tracks in the $B - P$ plane according to the rate at which matter is accreted from the companion, and the rate at which the magnetic field decays. The evolutionary tracks essentially fill all the space in the B-P plane, starting at our assumed initial condition of an old canonical pulsar with field of 10^{12} G, and extending downward in field strength, broadening to fill the space on both sides of the deathline, and extending to the small periods of millisecond pulsars. All are potential tracks of some particular binary pair, since accretion rates vary by several orders of magnitude and presumably so do decay rates of the magnetic field. As a first orientation as to our results and how they relate to known pulsars as regards their magnetic field strength and their rotational period, we show the evolutionary tracks for four different accretion rates given in units of $\dot{M} = 10^{-10}$ solar masses per year in Fig. 13. The decay rate of the magnetic field is taken to have the

value $t_d = 10^6$ yr in each case. The x-ray neutron star gains angular momentum and its period decreases, and over a longer timescale, the magnetic field decays. One can see already that a wide swathe of B and P is traced out.

In the above example, the field was assumed to decay to a finite asymptotic value of 10^8 Gauss. A very different assumption, namely that the field decays eventually to zero, $B(t) = B(0)e^{-t/t_d}$, modifies only the results below the asymptotic value, as is seen by comparing Fig. 13 and 14. However, the conclusion concerning the origin of millisecond pulsars is quite different. For purely exponential decay, one would conclude that high frequency pulsars are created only in high accretion rate binaries.

In the remainder of the paper, we assume the field decays to an asymptotic value, since from the above comparison we see how exponential decay would modify the picture.

We show time tags on a sample track in Fig. 15 which provides some sense of time lapse. The first part of a track is traversed in short time, but the remainder ever more slowly. This shows up also in dP/dt as a function of time. For each of

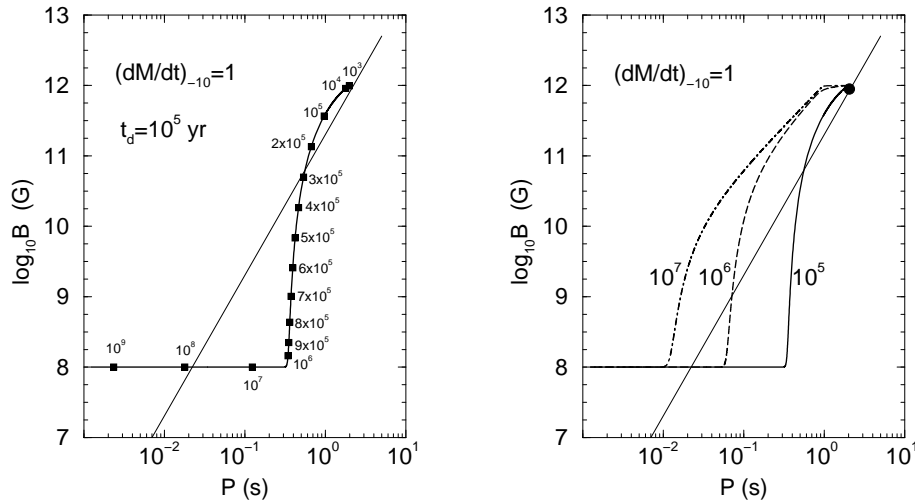


Fig. 15. Time tags expressed in years are shown for one of the evolutionary tracks corresponding to a decay constant for the magnetic field of $t_d = 10^5$ y.

Fig. 16. Evolutionary tracks for a neutron star starting at the death line and evolving by accretion to lower field and high frequency for an accretion rate 1 in units of 10^{-10} solar masses per year, and for three values of the magnetic field decay rate t_d as marked.

three accretion rates we show the dependence on three field decay constants in Figs. 16, 17 and 18. Depending on decay rate of the field and accretion rate, an X-ray neutron star may spend some time on either side of the death line, but if

it accreted long enough, always ends up as a candidate for a millisecond pulsar *if* the magnetic field decays to an asymptotic value such as was assumed. However, if the field decays exponentially to zero, only high accretion rates would lead to millisecond pulsars. Of course, if accretion turns off at some time, the evolution is arrested.

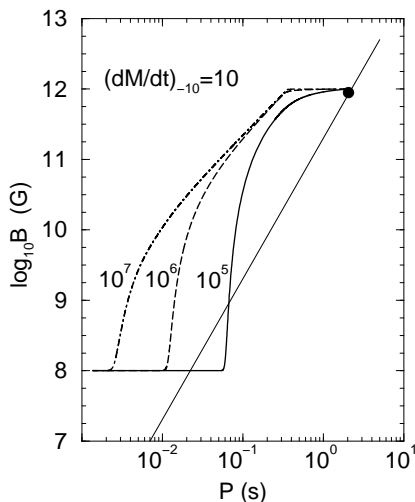


Fig. 17. Evolutionary tracks similar to Fig. 16 but with a different accretion rate $(dM/dt)_{-10} = 10$.

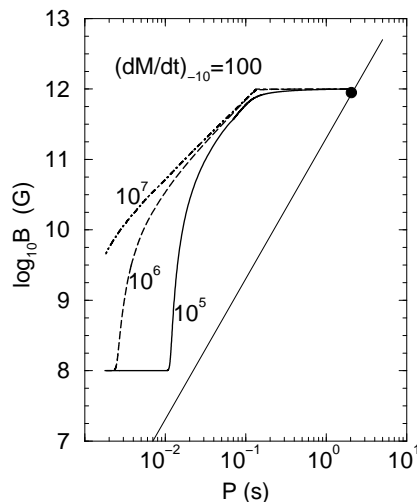


Fig. 18. Evolutionary tracks similar to Fig. 16 but with a different accretion rate $(dM/dt)_{-10} = 100$.

In summary, we have computed the evolutionary tracks in the $B - P$ plane due to mass accretion onto neutron stars beginning at the death line with a typical field strength of 10^{12} Gauss, to shorter periods and low fields. According to the assumed accretion rate and decay constant for the magnetic field, the tracks indicate that the individual binaries with characteristics ranging from Z to Atoll sources will evolve along paths that cover a broad swathe in the $B - P$ plane. These include tracks of X-ray stars corresponding to low accretion rates that follow a path beyond the death line in the so-called ‘graveyard’. We have assumed two particular forms for the law of decay of the magnetic field. (1) The field approaches an asymptotic value of 10^8 Gauss such as is typical of millisecond pulsars. This assumption leads to a particular form for the termination of evolutionary tracks. All accreters, no matter what the accretion rate, will end with millisecond periods, unless accretion ceases beforehand. (2) If instead, we had assumed a purely exponential decay, the tracks would not tend to an asymptotic value, but would continue to decrease in the strength of B .

The tracks would still cover a broad swathe in the $B - P$ plane. But one would conclude that only the higher accretion rate binaries, particularly the Z-sources, could produce millisecond period neutron stars. If accretion continues for too long a time, the neutron star will be carried to very low fields and across the death line, or an overcritical mass will have been accreted, leading instead to a black hole.

5 Appendices

5.1 First Order Phase Transition in Neutron Stars

We briefly recall some of the main characteristics of a first order phase transition in any substance having more than one conserved quantity, or as we will call it in the context of physics—conserved charge—such as baryon number or electric charge [38]. These are the two conserved quantities relevant to neutron stars. They have zero net electric charge and are made from baryons.

What makes a substance having more than one conserved charge different from a substance having only one, is that charges in the first case can be exchanged between two phases of the substance in equilibrium so as to minimize the energy. And the concentration of the charges can readjust at each proportion of the phases to minimize the energy. There is no such degree of freedom in a single-component substance, and there are $n - 1$ degrees of freedom in a substance having n independent components or conserved charges.

In a single-component substance, the pressure at constant temperature remains unaltered for all proportions of the two phases as the substance is compressed. Only the proportion of the phases changes. This is not so for a substance of more than one conserved charge. The degree(s) of freedom to readjust the concentrations of the charges at each proportion of the phases causes a change in all internal properties of the two phases as their proportion changes including their common pressure under conditions of constant temperature.

The fact that the pressure varies as the proportion of phases in equilibrium in neutron star matter has an immediate consequence. The mixed phase of two phases in equilibrium will span a finite radial distance in a star. If the pressure were a constant for all proportions, then the mixed phase would be squeezed out of the star because the pressure varies monotonically, being greatest at the center and zero at the edge of the star. In early work on phase transitions in neutron stars, they were always treated as having constant pressure at the zero temperature of the star, so the mixed phase never appeared in any of those models.

The difference in properties of first order phase transitions in a one-component substance and one with several independent components or conserved charges is easily proven. First consider a one-component substance for which equilibrium of two phases, A and B is expressed by

$$p_A(\mu, T) = p_B(\mu, T). \quad (21)$$

At constant T , the solution for the chemical potential is obviously unique and independent of the proportion of the phases. So all properties of the two phases remain unaltered as long as they are in equilibrium, no matter the proportion.

Now consider a substance having two conserved charges (or independent components). For definiteness we consider the two independent conserved charges of neutron star matter, baryon number and electric charge, whose densities we denote by ρ and q . For the corresponding chemical potentials we choose those of the neutron, μ_n , and electron, μ_e . The chemical potentials of all other particles can be written in terms of these independent ones. Gibbs phase equilibrium between the confined hadronic phase C and the deconfined quark matter phase D is now expressed as

$$p_C(\mu_n, \mu_e, T) = p_D(\mu_n, \mu_e, T). \quad (22)$$

This equation is insufficient to find the chemical potentials. At fixed T , it must be supplemented by another, say a statement of the conservation of one of the conserved charges. How should that statement be made? If one of the charges is the electric charge, demanding that the electric charge density should vanish identically in both phases would satisfy the condition of charge neutrality as required of a star.² That is in fact how charge neutrality in neutron stars was enforced for many years. However, it is overly restrictive. The net charge must vanish, but the charge density need not. Only the integrated electric charge density must vanish, $\int q(r)d^3r = 0$.³ We refer to this as global conservation rather than local. It releases a degree of freedom that the physical system can exploit to find the minimum energy. To express this explicitly, we note that according to the preparation of the system, whether in the laboratory, or in a supernova, the concentration of the charges is fixed when the system is in a single phase. Denote the concentration by

$$c = Q/B. \quad (23)$$

However, when conditions of temperature or pressure change to bring the system into two phases equilibrium, the concentrations in each can be different

$$c_C = Q_C/B_C, \quad c_D = Q_D/B_D \quad (24)$$

provided only that the total charges are conserved,

$$Q_C + Q_D = Q, \quad B_C + B_D = B. \quad (25)$$

Here Q and B denote the total electric and baryon charge in a volume V . The rearrangement of charges will take place to minimize the energy of the system. The force that is responsible for exploiting this degree of freedom in neutron

² The Coulomb force is so much stronger than the gravitational that the net charge per baryon has to be less than 10^{-36} which we can call zero.

³ Familiar examples of neutral systems that have finite charge densities of opposite sign are atoms and neutrons.

stars is the one responsible for the symmetry energy in nuclei and the valley of beta stability. Since neutron stars are far from symmetry, the symmetry energy is quite large; the difference in Fermi energies of neutron and proton, and the coupling of baryon isospin to the neutral rho meson are responsible.

For a uniform medium, and every sufficiently small region V in a neutron star is uniform to high accuracy, the statement of global conservation is

$$\int_{V_C} q_C(r) d^3r + \int_{V_D} q_D(r) d^3r = V_C q_C + V_D q_D = Q \quad (26)$$

where V_C and V_D denote the volume occupied by the two phases respectively. This can be written more conveniently as

$$(1 - \chi) q_C(\mu_n, \mu_e) + \chi q_D(\mu_n, \mu_e) = Q/V \equiv \bar{q} \quad (27)$$

where q_C denotes the density of the conserved charge in the confined phase, q_D in the deconfined phase, and

$$\chi = V_D/V, \quad V = V_C + V_D \quad (28)$$

is the volume proportion of phase D and \bar{q} is the volume averaged electric charge (which for a star is zero). Now, equations (22) and (27) are sufficient to find μ_n and μ_e . But notice that the solutions depend on the volume proportion χ . Therefore, also all properties of the two phases depend on their proportion, including the common pressure. Having solved for the chemical potentials (and all field quantities specified by their equations of motion), the densities of the baryon conserved charge in the phases C and D , are given by $\rho_C(\mu_n, \mu_e)$ and $\rho_D(\mu_n, \mu_e)$. The volume average of the baryon density is given by an equation corresponding to Eq. (27).

Let us now discuss the consequences of opening the degree of freedom embodied in Eq. (27), ie., in allowing electric charge (and strangeness) to be exchanged by the two phases in equilibrium so as to achieve the minimum energy at the corresponding baryon density. Because of the long range of the Coulomb force the Coulomb energy will be minimized when regions of like charge are small, whereas the surface interface energy will be minimized when the surface areas of the regions of the two phases is small. These are opposing tendencies, and in first order can be reconciled by minimizing their sum. A Coulomb lattice will form [38] of such a size and geometry of the rare phase immersed at spacings [39,40] in the dominant phase so as to minimize the energy.

In better approximation, the total energy, consisting of the sum of bulk energies, the surface and Coulomb energies and higher corrections such as the curvature energy,

$$E_{\text{Total}} \approx E_{\text{Bulk}} + E_{\text{Surface}} + E_{\text{Coulomb}} + E_{\text{Curvature}} + \dots, \quad (29)$$

should be minimized. In still better approximation, the convenient partition of the energy as above would be replaced by a lattice calculation of the total energy [41]. In general, the opening of the degree(s) of freedom to conserve charges

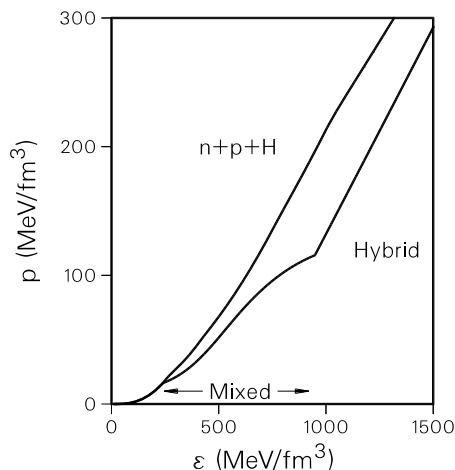


Fig. 19. Equation of state for a first order phase transition from neutron star matter in its confined to deconfined phases (marked hybrid). Note the monotonically increasing pressure. Comparison is made with the equation of state of neutron star matter in the confined phase with nucleons hyperons and leptons in equilibrium.

globally rather than locally, or any other arbitrary way, can only lower the total energy from the value it would have were the degree of freedom closed, or in very special cases leave it unchanged. However, in the case of a neutron star, the degree of freedom allows the bulk energy in the normal phase to be lowered by decreasing the charge asymmetry of neutron star matter, so exchange of charge between the confined and deconfined phases is evidently favorable. It is unphysical to choose an arbitrary value of surface tension such that the mixed phase is energetically unfavored. The surface tension should be *calculated self-consistently* by minimizing the total energy Eq. (29), when possible [42].

However, our purpose here is not to calculate the geometric structure⁴ of the mixed phase but to exhibit the equation of state for a first order deconfinement transition in neutron star matter according to the above principles. Fig. 19 shows the equation of state with the pure phases at low and high density and the mixed phase between. Note, as pointed out before that though the phase transition is first order, having as it does a mixed phase, the pressure (and all other internal properties) vary with density. The monotonic increase of pressure contrasts with early treatments of phase transitions in neutron stars prior to 1991, for which approximations rendered a constant pressure in the mixed phase [43]. For a constant pressure phase transition, gravity will squeeze out the mixed phase. Pressure is a monotonically decreasing function of distance from the center of a star, just as it is in our atmosphere.

⁴ See Ref. [47] for a review.

5.2 Description of the Confined and Deconfined Phases

To describe the confined phase of neutron star matter, we use a generalization [44] of relativistic nuclear field theory solved at the mean field level in which nucleons and hyperons (the baryon octet) are coupled to scalar, vector and vector-isovector mesons. A full description of how the theory can be solved for neutron star matter can be found in [5,44]. The Lagrangian is

$$\begin{aligned}
\mathcal{L} = & \sum_B \bar{\psi}_B (i\gamma_\mu \partial^\mu - m_B + g_{\sigma B} \sigma - g_{\omega B} \gamma_\mu \omega^\mu \\
& - \frac{1}{2} g_{\rho B} \gamma_\mu \boldsymbol{\tau} \cdot \boldsymbol{\rho}^\mu) \psi_B + \frac{1}{2} (\partial_\mu \sigma \partial^\mu \sigma - m_\sigma^2 \sigma^2) \\
& - \frac{1}{4} \omega_{\mu\nu} \omega^{\mu\nu} + \frac{1}{2} m_\omega^2 \omega_\mu \omega^\mu - \frac{1}{4} \rho_{\mu\nu} \cdot \rho^{\mu\nu} + \frac{1}{2} m_\rho^2 \rho_\mu \cdot \rho^\mu \\
& - \frac{1}{3} b m_n (g_\sigma \sigma)^3 - \frac{1}{4} c (g_\sigma \sigma)^4 \\
& + \sum_{e^-, \mu^-} \bar{\psi}_\lambda (i\gamma_\mu \partial^\mu - m_\lambda) \psi_\lambda.
\end{aligned} \tag{30}$$

The summ on B is over all charge states of the baryon octet. The parameters of the nuclear Lagrangian can be algebraically determined (see 2nd ed. of [5]) so that symmetric nuclear matter has the following properties: binding energy of symmetric nuclear matter $B/A = -16.3$ MeV, saturation density $\rho = 0.153$ fm⁻³, compression modulus $K = 300$ MeV, symmetry energy coefficient $a_{\text{sym}} = 32.5$ MeV, nucleon effective mass at saturation $m_{\text{sat}}^* = 0.7m$ and ratio of hyperon to nucleon couplings $x_\sigma = 0.6$, $x_\omega = 0.653 = x_\rho$ that yield, together with the foregoing parameters, the correct Λ binding in nuclear matter [45].

Quark matter is treated in a version of the MIT bag model with the three light flavor quarks ($m_u = m_d = 0$, $m_s = 150$ MeV) as described in Ref. [46]. A value of the bag constant $B^{1/4} = 180$ MeV is employed.

Acknowledgments: This work was supported by the Director, Office of Energy Research, Office of High Energy and Nuclear Physics, Division of Nuclear Physics, of the U.S. Department of Energy under Contract DE-AC03-76SF00098. F. Weber was supported by the Deutsche Forschungsgemeinschaft.

References

1. M. A. Alpar, A. F. Cheng, M. A. Ruderman and J. Shaham, *Nature* **300** (1982) 728.
2. D. Bhattacharya and E. P. J. van den Heuvel, *Phys. Rep.*, **203** (1991) 1.
3. R. Wijnands and M. van der Klis, *Nature* **394** (1998) 344.
4. D. Chakrabarty and E. H. Morgan, *Nature* **394** (1998) 346.

5. N. K. Glendenning, *COMPACT STARS* (Springer-Verlag New York, 1st ed. 1996, 2nd ed. 2000).
6. N. K. Glendenning, S. Pei and F. Weber, *Phys. Rev. Lett.* **79** (1997) 1603.
7. N. K. Glendenning, *Nucl. Phys.* **A638** (1998) 239c.
8. H. Heiselberg and M. Hjorth-Jensen, *Phys. Rev. Lett.* **80** (1998) 5485.
9. E. Chubarian, H. Grigorian, G. Poghosyan and D. Blaschke, *Astron. Astrophys.* **357** (2000) 968.
10. F. Pacini, *Nature* **216** (1967) 567.
11. N. K. Glendenning and F. Weber, *Astrophys. J.* **400** (1992) 647.
12. F. Weber and N. K. Glendenning, *Astrophys. J.* **390** (1992) 541.
13. A. Johnson, H. Ryde and S. A. Hjorth, *Nucl. Phys.* **A179** (1972) 753.
14. F. S. Stephens and R. S. Simon, *Nucl. Phys.* **A183** (1972) 257.
15. B. R. Mottelson and J. G. Valatin, *Phys. Rev. Lett.* **5** (1960) 511.
16. N. K. Glendenning and F. Weber, astro-ph/0003426, (2000).
17. M. van der Klis, Millisecond Oscillations in X-Ray Binaries, to appear in *Ann. Rev. Astron. Astrophys.*, (2000).
18. R. F. Elsner and F. K. Lamb, *Astrophys. J.* **215** (1977) 897.
19. P. Ghosh, F. K. Lamb and C. J. Pethick, *Astrophys. J.* **217** (1977) 578.
20. V. M. Lupinov, *Astrophysics of Neutron Stars*, (Springer-Verlag, New York, 1992).
21. S. Konar and D. Bhattacharya, *MNRAS* **303** (1999) 588; op. cit. **308** (1999) 795.
22. J. B. Hartle, *Astrophys. J.* **150** (1967) 1005.
23. J. B. Hartle and K. S. Thorne, *Astrophys. J.* **153** (1968) 807.
24. F. Weber, *J. Phys. G: Nucl. Part. Phys.* **25** (1999) R195.
25. I. Tanihata, *Prog. Part. Nucl. Phys.* **35** (1995) 505.
26. P. G. Hansen, A. S. Jensen and B. Johnson, *Ann. Rev. Nucl. Part. Sci.* **45** (1997) 1644.
27. Bao-An Li, C. M. Ko and Zhongzhou Ren, *Phys. Rev. Lett.* **78** (1997) 1644.
28. L. Bildsten, *Astrophys. J.* **501** (1998) L89.
29. N. Anderson, D. I. Jones, K. D. Kokkotas and N. Sterigioulas, *Astrophys. J.* **534** (2000) L89.
30. Y. Levin, *Astrophys. J.* **517** (1999) 328.
31. N. K. Glendenning and F. Weber, astro-ph/0010336 (2000).
32. V. A. Urpin and U. Geppert, *MNRAS* **278** (1996) 471.
33. V. A. Urpin and D. Konenkov, *MNRAS* **284** (1997) 741.
34. V. A. Urpin, U. Geppert and D. Konenkov, *MNRAS* **295** (1998) 907.
35. M. Salgado, S. Bonazzola, E.ourgoulhon and P. Haensel, *Astron. Astrophys.* **291** (1994) 155.
36. G. B. Cook, S. L. Shapiro and S. A. Teukolsky, *Astrophys. J. Lett.* **423** (1994) L117; op. cit. **424** (1994) 823.
37. L. Burderi, M. Colpi, T. Di Salvo, N. D'Amico, *Astrophys. J.* **519** (1999) 285.
38. N. K. Glendenning, *Nucl. Phys. B (Proc. Suppl.)* **24B** (1991) 110; *Phys. Rev. D* **46** (1992) 1274.
39. N. K. Glendenning and S. Pei, *Phys. Rev. C* **52** (1995) 2250.
40. N. K. Glendenning and S. Pei, in the Eugene Wigner Memorial Issue of Heavy Ion Physics (Budapest) **1** (1995) 1.
41. R. D. Williams and S. E. Koonin, *Nucl. Phys.* **A435** (1985) 844.
42. M. Christiansen, N. K. Glendenning and J. Schaffner-Bielich, *Phys. Rev. C* **62** (2000) 025804.
43. N. K. Glendenning, *Phys. Rev. D* **46** (1992) 1274.
44. N. K. Glendenning, *Astrophys. J.* **293** (1985) 470.
45. N. K. Glendenning and S. A. Moszkowski, *Phys. Rev. Lett.* **67** (1991) 2414.
46. E. Farhi and R. L. Jaffe, *Phys. Rev. D* **30** (1984) 2379.
47. N. K. Glendenning, *Phys. Rep.* **342** (2001) 393.